Capillary ripples on standing water waves

Lei Jiang, William W. Schultz, and Marc Perlin

Department of Mechanical Engineering and Applied Mechanics
Department of Naval Architecture and Marine Engineering
University of Michigan, Ann Arbor, Michigan 48109 USA

The dynamics of capillary-gravity standing waves strongly impact remote sensing. Satellite images obtained by SAR (Synthetic Aperture Radar) exhibit brighter radar returns near ocean features such as currents, shelves, and slicks. The backscatter of microwaves by these surface features is sensitive to the curvature and periodicity of the sea surface on centimeter scales. Dynamics of wave reflection in these regions and hence the dynamics of standing waves are critical in interpreting SAR images. Jiang *et al.* (1996) generated Faraday waves in laboratory experiments and compared to fully-nonlinear numerical simulations. New dynamics of harmonic interaction and interesting steep waves were discovered. In particular, triply-periodic breaking are discussed in Jiang *et al.* (1997). Herein, we present results on even shorter wavelengths, 2 cm to 15 cm, and on the formation of superharmonic waves (ripples) in the ensuing wave forms.

Numerical methods and experimental techniques

The flow is assumed to be irrotational, spatially periodic, and infinitely deep. Capillary number $\kappa = \sigma k^2/\rho g$ represents the effect of surface tension, where σ is the surface tension, k is the wavenumber, ρ is the water density, and g is the gravitational acceleration. The fully-nonlinear free surface problem is solved by a spectral Cauchy-integral method, based on the kernel desingularization of Roberts (1983). As shown in Schultz *et al.* (1994), this method gives exponentially accurate solutions. When vertical forcing is provided, a term proportional to ϕ_{xx} is added to the dynamic free surface condition to simulate the free-surface boundary-layer damping and to provide an energy sink to balance the wave forcing.

The standing wave excited by vertical oscillation (Faraday resonance) is subharmonic (Benjamin & Ursell 1954). Herein Faraday resonance is used as a "clean" experimental method to generate two-dimensional steep standing waves. We use a rectangular glass tank 105 mm long and 300 mm deep. The testing water depth is 150 mm in the experiments. An aspect ratio of 6.2 : 1 in the third dimension is chosen to eliminate cross waves and maintain a two-dimensional wave field. The wave profile is recorded with a laser-sheet technique and a high-speed intensified imager/recorder. The vertical oscillation is provided by a mechanical shaker with computer control.

Parasitic ripple generation

We first validate our numerical method by calculating parasitic ripple formation on the forward face of traveling gravity waves (Cox 1958, Longuet-Higgins 1963). A linear Stokes wave is used as the initial condition with wavelengths of 6.5 cm ($\kappa = 0.07$) and 5 cm ($\kappa = 0.119$). The wave first becomes spatially asymmetric with the crest tilting forward (wave steepness ka=0.20). Then larger curvature is found on the forward face and ripples are excited after one wave period, as shown in figure 1. The number of ripples and their large steepness agree with the experiments by Perlin *et al.* (1993) and the viscous simulation of Dommermuth (1994). These computations prove that neither viscous damping nor vorticity is required for the ripple formation, even though damping may be needed to describe the subsequent evolution of these parasitic ripples and the underlying vortex structure (Longuet-Higgins 1992, Mui & Dommermuth 1995). Demonstrating ripple formation requres only 64 free-surface nodes per wave length in our computation; much more efficient than Dommermuth's full-field computation.

Ripple formation can be interpreted as higher-order resonance between the fundamental mode and its superharmonics at critical capillary numbers $\kappa = 1/N$ (Wilton 1915) where N is an integer. Longuet-Higgins (1963) explained parasitic ripples on a traveling wave as the result of a capillarity-induced pressure disturbance at the wave crest, analogous to ripple generation on a *steady* stream. Because the group velocity for capillary waves is faster than the phase velocity of the underlying wave, the ripples appear on the front face of the wave crest. Ripple formation cannot be confirmed by Longuet-Higgins' theory for standing waves, as the standing wave is *unsteady* and the background flow can no longer be transformed into a *steady* stream. However, the high-order resonance condition: $\kappa = 1/N$ should be equally valid for traveling waves and standing waves, therefore predicting ripple formation on standing waves.

Our numerical simulation for free standing waves uses a high-order gravity standing wave solution as the initial condition. A large-amplitude 6.5-cm wave (ka=0.57) evolves into a waveform with many ripples on the surface. Shown in figure 2, the number of ripples is about 15 ($\approx 1/\kappa$). The ripple growth can be explained in terms of interaction between short waves and a long wave as follows: Curvature variations first appear at the crest during its ascending phase. When the crest motion reverses, small ripples are carried by the orbital velocity of the underlying wave to the two troughs with their wavelength stretched and their steepness reduced. Because capillary waves propagate faster, these ripples reach the two troughs before the orbital velocity reverses. The ripples then encounter an opposing velocity field and are shortened and steepened. This *intermittent* growth occurs within one half wave cycle. Compared to traveling waves, the ripple growth is slower and the average ripple steepness is much smaller, although the initial wave steepness is three times larger. The ripples are generally shorter and steeper at the trough of a standing wave (figure 2b), in contrast to the behavior of short waves on a long traveling wave.

In reality, water waves are accompanied by a free-surface boundary layer that provides a viscous damping proportional to the square of wavenumber. The higher harmonics experience much larger damping than the fundamental harmonic. Therefore, the already weak parasitic ripples can be suppressed by viscous damping. We model both vertical forcing (acceleration) and viscous damping (ϕ_{xx} term) to simulate Faraday waves. A periodic wave solution is achieved with the same wave steepness and the same κ as shown in figure 2. However, due to the viscous damping, ripples form and decay quickly before significant ripple steepness is reached.

Using Faraday resonance, we generate 10.5-cm Faraday waves ($\kappa = 0.0265$) in laboratory experiments. These waves reach a maximum steepness of ka=1.32 with a rounded crest and very steep slope without parasitic ripples (figure 3). This large wave steepness and the corresponding wave profile agree with the calculations of Schultz & Vanden-Broeck (1990) for free standing waves. More extensive experiments on wavelengths from 5 cm to 10 cm are required to further confirm our numerical findings on the parasitic ripples and the effect of viscous damping.

Wilton ripples under Faraday resonance

Internal resonance occurs at the critical capillary number $\kappa = 1/N$, leading to the existence of a family of solutions (Wilton ripples). Only limited modes participate in the resonance when N is a small integer. Generalized Wilton ripples are usually referred to as triad interactions (Perlin *et al.* 1990). For standing waves with $\kappa = 1/2$, two solutions are found for moderate wave amplitude by Vanden-Broeck (1984). Both the first and the second harmonics are retained at first order in his analysis. However, such solutions are limited by the weakly-nonlinear assumption, leaving the behavior of capillary-gravity standing waves at large wave steepness unexplored.

We calculate standing waves generated by Faraday resonance at these critical capillary numbers. The wavelength is fixed at 2.44 cm ($\kappa = 1/2$). With small forcing amplitude, we obtain a periodic wave with low wave steepness (ka=0.06) in figure 4(a). Either one crest or two crests appear at different phases of a wave cycle, similar to the two solutions of Vanden-Broeck (1984). As we increase the forcing amplitude and therefore increase the wave steepness to ka=0.35 (figure 4b), three or four crests appear in the wave profile at different phases of a periodic wave cycle. A frequency spectrum of wave elevation demonstrates that the second, the third, and the fourth harmonics are equally significant (the fundamental harmonic is 9.8 Hz). This behavior is not described by the two-mode model of Henderson & Miles (1991) for 2:1 resonance in Faraday waves.

The appearance of higher harmonics is even more evident for $\kappa = 1/3$. With a fixed forcing amplitude and forcing frequency in our numerical calculations, shorter and shorter ripples appear in a cascade on the free surface, and a periodic state is never reached. If the forcing frequency is slightly different from twice the linear natural frequency, we observe quasi-periodic and chaotic motions in the surface elevation. The cascade to higher wavenumbers eventually leads to a wavelength on the scale of the node spacing and our computation fails.

This proliferation of superharmonics for capillary-gravity waves appears to be not studied in detail in the literature. Perlin & Ting (1992) noted multiple crests in traveling Wilton ripples directed excited by a wavemaker. The importance of small-scale wave forms to remote sensing applications warrants a more in-depth study of these phenomena.

This research was supported by the Office of Naval Research partially under contract number N00014-93-1-0867 and partially under the University Research Initiative Ocean Surface Processes and Remote Sensing at the University of Michigan, contract number N00014-92-J-1650.

References

Benjamin, T. B. & Ursell, F. 1954 The stability of the plane free surface of a liquid in vertical periodic motion.*Proc. R. Soc. Lond.* A **225**, 505–515.

Cox, C. S. 1958 Measurements of slopes of high-frequency wind waves. *J. Mar. Res.* **213**, 95–109.

Dommermuth, D. G. 1994 Efficient simulation of short and long-wave interactions with applications to capillary waves. *ASME J. Fluid Eng.* **116** (1), 77–82.

Henderson, D. M. & Miles, J. W. 1991 Faraday waves in 2:1 internal resonance. *J. Fluid Mech.* **222**, 449–470.

Jiang, L.,Ting, C.-L., Perlin, M. & Schultz, W. W. 1996 Moderate and steep Faraday waves: Instabilities, modulation and temporal asymmetries. *J. Fluid Mech.* **329**, 275–307.

Jiang, L., Perlin, M. & Schultz, W. W. 1997 An experimental study of breaking standing waves: period tripling and breaking-wave dissipation. Submitted for publication.

Longuet-Higgins, M. S. 1963 The generation of capillary waves by steep gravity waves. *J. Fluid Mech.* **16**, 138–159.

Longuet-Higgins, M. S. 1992 Capillary rollers and bores. *J. Fluid Mech.* **240**, 659–679.

Mui, R. C. Y. & Dommermuth, D. G. 1995 The vortical structure of parasitic capillary waves. *ASME J. Fluid Eng.* **117** (3), 355–61.

Perlin, M., Henderson, D. & Hammack, J. 1990 Experiments on ripple instabilities. 2. Selective amplification of resonant triads. *J. Fluid Mech.* **219**, 51–80.

Perlin, M., Lin, H. & Ting, C. 1993 On parasitic capillary waves generated by steep gravity waves: an experimental investigation with spatial and temporal measurements. *J. Fluid Mech.* **255**, 597–620.

Perlin, M. & Ting, C.-L. 1992 Steep gravity-capillary waves within the internal resonance regime. *Phys. of Fluids A* **4** (11), 2466–2478.

Roberts, A.J. 1983 A stable and accurate numerical method to calculate the motion of a sharp interface between fluids *IMA J. Appl. Math.* **31**.

Schultz, W. W., Huh, J. & Griffin, O. M. 1994 Potential energy in steep and breaking waves. *J. Fluid Mech.* **278**, 201–228.

Schultz, W. W. & Vanden-Broeck J. M. 1990 Computations of nonlinear standing waves. *Bull. Amer. Phys. Soc.* **35**, 2290.

Schultz, W. W., Vanden-Broeck J. M., Jiang, L. & Perlin, M. 1996 Nonlinear standing waves: singularity formation and small surface tension effect. Submitted for publication.

Vanden-Broeck, J. M. 1984 Nonlinear gravity-capillary standing waves in water of arbitrary uniform depth. *J. Fluid Mech.* **139**, 97–104.

Wilton, J. R. 1915 On ripples. *Phil. Mag.* **29** (6), 688–700.

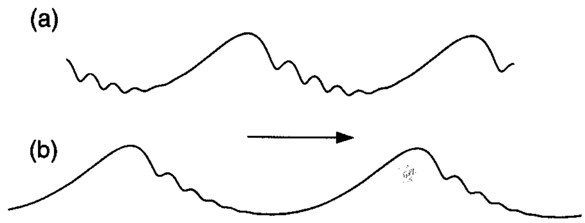

Figure 1: Calculated parasitic ripples on traveling wave (ka=0.20) with wavelengths (a) 5 cm, (b) 6.5 cm.

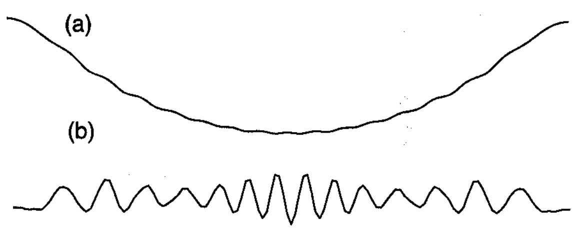

Figure 2: Calculated 6.5-cm standing wave (ka=0.57) with parasitic ripples, (a) elevation, (b) curvature.

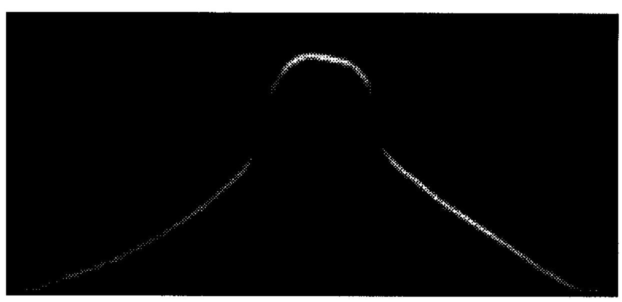

Figure 3: Laser-sheet image of steep (ka=1.23) Faraday wave of 10.5-cm wavelength.

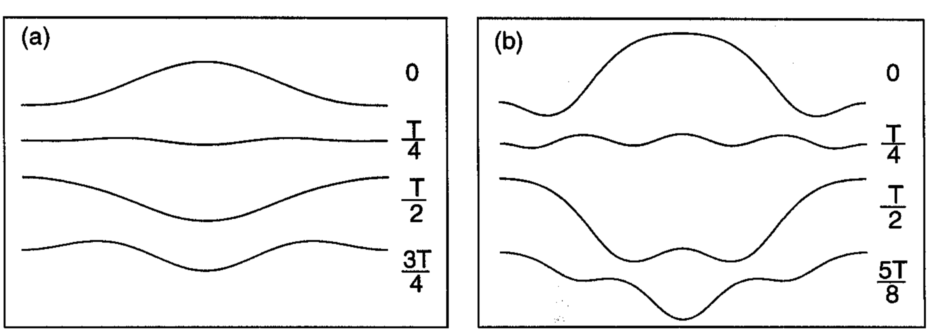

Figure 4: Calculated Faraday wave at different phases of the wave period T for $\kappa = 1/2$ (wavelength: 2.44 cm). (a) ka=0.06, forcing amplitude: 0.045 mm; (b) ka=0.35, forcing amplitude: 0.12 mm.

DISCUSSION

Grilli S.: You mentioned that to model laboratory experiments, you used a φ_{xx} damping term. Would this be also applicable to the real ocean?

Jiang L., Schultz W., Perlin M.: We use the φ_{xx} damping term to model open ocean where free-surface boundary layer is the dominant source of dissipation. Damping measured in laboratory experiments is dominated by the sidewall boundary layer and contact-line damping. A good model that consider all these effects has not yet been found.

Wu T.Y.: Taylor seems to have objected to the 90-degree conjecture.

Jiang L., Schultz W., Perlin M.: Yes, Taylor (1953) questioned the derivations for the 90-degree conjecture, even though he did not say the conjecture was wrong. However, his experiments did not disapprove the conjecture. We have found a crest angle smaller than 90 degrees in calculation. In the experiments where period-tripled breaking occurs, the sharp-crest mode has a crest angle much less than 90 degrees.